

Direct wiring of carbon nanotubes for integration in nanoelectromechanical systems

S. Bauerdick^{a)} and A. Linden

Raith, Research and Development, Hauert 18, 44227 Dortmund, Germany

C. Stampfer, T. Helbling, and C. Hierold

Micro and Nanosystems, ETH Zurich, 8092 Zurich, Switzerland

(Received 31 May 2006; accepted 9 October 2006; published 4 December 2006)

The authors present the use of electron beam induced deposition (EBID) for direct wiring of carbon nanotubes (CNTs). Since this technique is a maskless, direct patterning method, EBID is applicable to suspended nanotubes potentially integrated in predefined nanoelectromechanical systems (NEMS). The authors developed a process including CNT adsorption from solution on prepatterned planar samples, evaluation and localization of CNTs by scanning force microscopy, preparation of GDSII layouts, and contacting CNTs by EBID of tungsten. EBID was performed in an integrated e-beam lithography and nanoengineering workstation using tungsten hexacarbonyl as precursor. With well controlled exposure conditions, a resistivity on the order of $10^{-2} \Omega \text{ cm}$ has been achieved. Moreover, electrical measurements on CNTs contacted by EBID tungsten leads clearly show transistorlike behavior. First tests on EBID metal lead integration on alumina NEMS structures were carried out. Thus EBID can enable a top metallization of CNTs on suspended NEMS structures, which should enhance also the mechanical stability between the lead and the CNT. © 2006 American Vacuum Society. [DOI: 10.1116/1.2388965]

I. INTRODUCTION

The integration of carbon nanotubes (CNTs) in nanomechanical¹ or nanoelectromechanical systems² (NEMS) has attracted increasing interest over the last decade. This is partially due to the potential of CNT (Ref. 3) based nanostructures for low power, highly sensitive, ultrafast devices.⁴ Actually, first demonstrations of carbon nanotube based switches⁵ and mass⁶ and pressure sensors⁷ have been recently presented. From a fundamental point of view, nanomechanical (and nanoelectromechanical) test benches may moreover provide the means to explore the classical and nonclassical mechanical (and subsequently electromechanical) properties of various nanostructures (e.g., nanotubes or nanowires). In both cases, the successful integration (in terms of mechanical fixation and electrical connection) of the nanostructure itself is highly crucial and is becoming increasingly challenging especially when moving towards connection of suspended structures (e.g., suspended carbon nanotubes grown by chemical vapor deposition^{8,9}).

Here we report on electron beam induced deposition (EBID) for direct contacting of carbon nanotubes with the future potential for electrical connection and integration of suspended CNTs. EBID (Refs. 10–12) is basically a localized chemical vapor deposition (CVD) where precursor molecules are adsorbed on the sample surface and resolved by electron beam irradiation into a solid nanostructure (e.g., conductive wires) and volatile by-products. Thus it is a maskless procedure to circumvent standard wet chemical lithography techniques (combined with lift-off process), which

are commonly used to contact nanotubes resting on substrates. Moreover, EBID is one of a few other (e.g., focused ion beam based deposition¹³) very promising techniques to directly contact suspended structures integrated in nanoelectromechanical structures. This article is organized as the following: In Sec. II we characterize different wires made by EBID technique under different settings. Section III focuses on the EBID assisted “maskless” contacting of carbon nanotubes and their electrical characterization. Finally we show in Sec. IV the feasibility of direct EBID on prereleased alumina based nanoelectromechanical structures.

II. ELECTRICAL CHARACTERIZATION OF EBID TUNGSTEN LEADS

In a first step we characterized different EBID tungsten wires. Therefore we made use of electron beam (e-beam) lithography and standard lift-off to predefine gold fingers (approximately 500 nm wide, 50 nm gold, and 1 nm chromium in thickness) sitting on 200 nm of silicon oxide [see Fig. 1(a1)]. On top of the fingers the EBID tungsten wires have been deposited in order to allow two and four point I - V characterization of the EBID wires under investigation. All EBID processes were carried out in an integrated e-beam lithography and nanoengineering workstation (Raith eLiNE) using tungsten hexacarbonyl as precursor. The base chamber pressure was 1.2×10^{-6} mbar and increased to 3.5×10^{-6} mbar with gas injection. The electron energy was set to 3 kV, and two different probe currents of 150 and 590 pA were tested. A step size of 20 nm and meander mode for exposure was used, and beam dwell times, i.e., the beam times per exposure dot, in the range of 30–300 ms were investigated.

^{a)}Author to whom correspondence should be addressed; electronic mail: bauerdick@raith.de

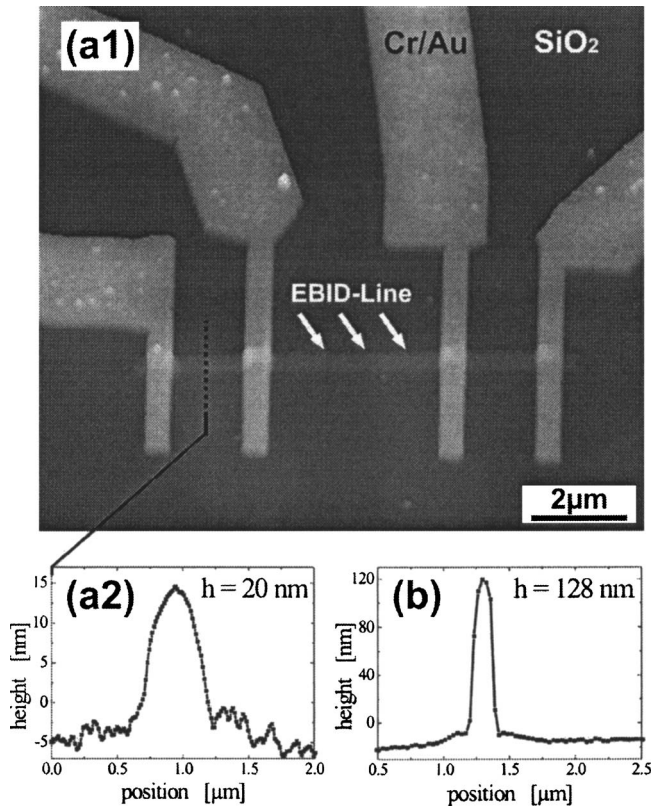


FIG. 1. Scanning force microscope measurements of EBID rectangles used for conductivity tests. Line scans are shown for a 380 nm wide EBID line (a2) fabricated with 60 ms dwell time (overview shown in (a1)) and a 70 nm wide EBID line (b) fabricated with 300 ms.

The examined EBID rectangles exhibit a designed length of 9 μm and a width varying from 60 to 400 nm due to the number of single pixel lines ranging between 2 and 20 [e.g., Figs. 1(a1) and (a2)]. Typical resistance values of such a deposited line are in the range of several 10–100 k Ω and a few 10 k Ω using the small (150 pA) and high probe (590 pA) current, respectively. Scanning force microscope (SFM) analysis (Fig. 1) shows a height of approximately 20 nm for the wide one [150 pA beam current, 20 single pixel lines, 60 ms dwell time, Fig. 1(a2)] and 130 nm for the narrow rectangle [150 pA beam current, 2 single pixel lines, 300 ms dwell time, Fig. 1(b)]. It is noteworthy that SFM images of rectangles deposited with higher probe currents showed blurred profiles and could not be measured accurately.

Results from electrical two and four point measurements are summarized in Table I. We observe Ohmic contacts and a metallic transport characteristic. In Fig. 2 we plot an example of a four point I - V characteristic measured on narrow (128 nm high) EBID tungsten wire (see insert in Fig. 2) leading to a resistance of approximately 17 k Ω . In summary we find that using a 150 pA e-beam current, a resistivity of 2.7×10^{-2} – $4.5 \cdot 10^{-3}$ Ω cm was extracted, assuming a rectangular shape of the EBID lines, whereas the highest dwell time, i.e., the beam time per exposure dot, gave the best conductivity. This is quite characteristic of tungsten hexacar-

TABLE I. Results for EBID resistance obtained with tungsten hexacarbonyl and a probe current of 150 pA at 3 kV for various exposure dwell times.

EBID parameters	60 ms/20 \times	300 ms/2 \times
Width (nm)	380	70
Height (nm)	18	128
R (k Ω)	700	500
(two point, 8 μm)		
R (k Ω)	160	20
(four point, 4 μm)		
Resistivity (Ω cm)	2.7×10^{-2}	4.5×10^{-3}

bonyl and could be explained by an improved volatility of the by-products. Moreover a transformation of the tungsten-carbon matrix from a loose to a less resistive state induced by the higher dwell time might occur.

III. RESULTS ON EBID CONTACTED CNTs ADSORBED ON SiO₂

A. Fabrication process

For electrical I - V measurements on carbon nanotubes using EBID wiring, we started with a highly doped silicon/silicon oxide sample with an oxide thickness of 200 nm. Gold electrodes (1 nm Cr and 40 nm Au) and reference alignment markers were prepatterned using standard e-beam lithography and lift-off technique.¹⁴ Single-walled CNTs fabricated by a high pressure CO conversion process¹⁵ have been dispersed in sodium dodecyl sulfate and are randomly adsorbed on the SiO₂ surface. SFM imaging is used to find location and orientation of the CNTs relative to the reference alignment markers. A mask layout for the following EBID leads is subsequently designed, reference Fig. 3(a). Then EBID of tungsten was applied for connecting the outer gold electrodes and CNTs. Since e-beam to sample position drift is induced by charging effects at the insulating SiO₂ surface,

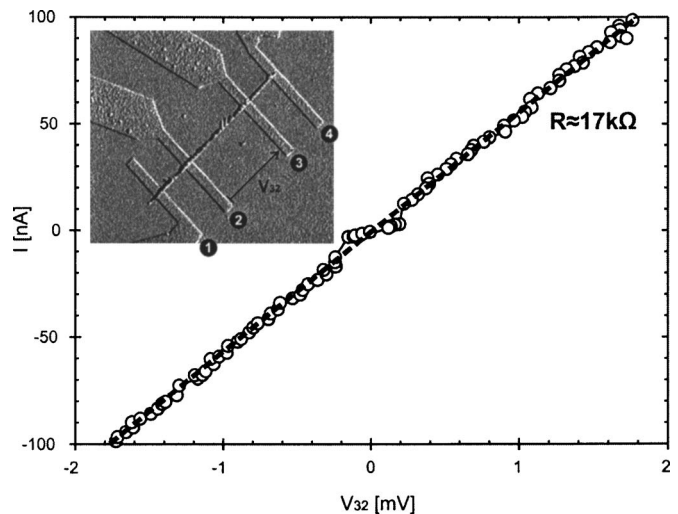


FIG. 2. I - V characteristic of a 70 nm wide EBID rectangle (see insert) exposed using a dwell time of 300 ms measured by a four point resistance measurement technique.

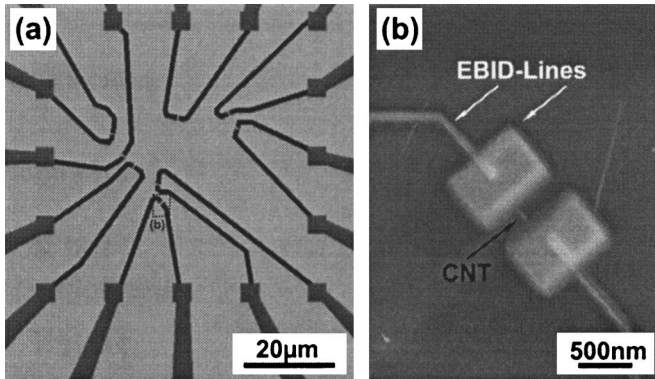


Fig. 3. GDSII design (a) and a scanning electron microscope (SEM) micrograph (b) illustrating the EBID wiring process for a CNT. Automatic drift compensation enables a precise definition of the contact position even at low beam energies on an insulating surface.

automatic drift compensation enables a precise definition of the contact position even at low beam energies. This compensation is achieved by an automatic coordinate offset correction using reference markers [e.g., cross on the left side of Fig. 4(a)] and is performed intermediately during the deposition process. The results are shown in Figs. 3 and 4, where the carbon nanotubes are also visible in the secondary electron image.

B. Electrical measurements on CNTs

The fabrication process described above has been used to contact several CNTs with two and three point EBID contacts (Fig. 4). We used the EBID process described in Sec. II, with a probe current of 140 pA and a dwell time of 300 or 400 ms, resulting in a width of the EBID lines of 120 nm. The three point setup [Fig. 4(b)] has been used for investigating the I - V characteristics of the contacted CNT. We applied a drain voltage (V_D) to the left contact [see Fig. 4(b)] and measured the source voltage (V_S) and the source-drain current (I_{DS}) at the center and right contact, respectively. The highly doped silicon substrate serves as the back gate and the 200 nm thick silicon oxide as the gate oxide. In Fig. 5 we show the electrical measurements of the CNT with three EBID contacts exhibiting transistorlike behavior. Both the

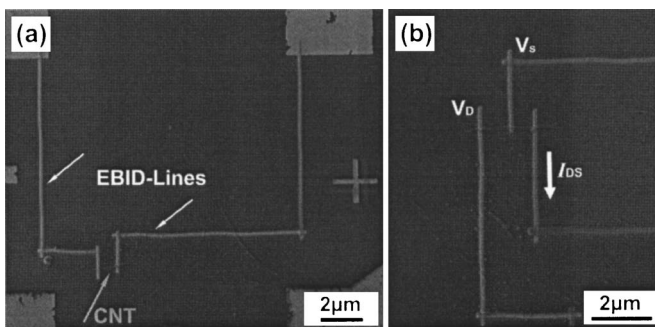


Fig. 4. SEM micrographs showing a two (a) and a three point (b) wiring of CNTs fabricated by EBID. The three point wiring has been used for the measurements given in Fig. 5.

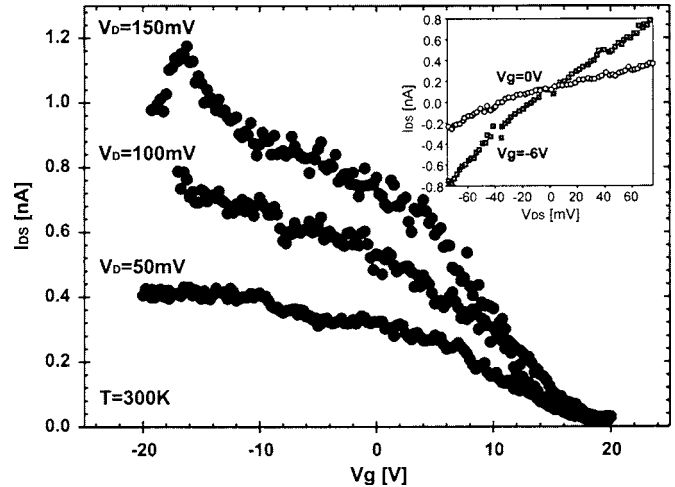


Fig. 5. Transistor characteristics of the CNT shown in Fig. 4(b) using EBID wiring, three point measurement, and a back gate (200 nm SiO_2). Source-drain current vs gate voltage for various drain voltages is shown. The insert shows source-drain current vs voltage for various gate voltages.

current-voltage characteristics (insert of Fig. 5) and the source-drain current dependency of the CNT on the applied gate voltage (Fig. 5) can be clearly observed. Please note that both EBID leads influence the source-drain current, whereas the voltage drop between V_D and V_S only includes one EBID lead.

IV. EBID OF CONDUCTIVE WIRES ON SUSPENDED NANOMECHANICAL STRUCTURES

The EBID technique described in Sec. II has also been used to examine the applicability of direct wiring on suspended nanomechanical structures. For this feasibility study we made use of prefabricated alumina based nanomechanical structures, which have been designed to investigate future NEMS devices. For the fabrication of the alumina based NEMS core structures, please refer to Refs. 16 and 17. Figure 6(a) shows a schematic illustration of the principle of such a possible NEMS device. A suspended Al_2O_3 comb drive structure can be moved in one direction by applying an electrical field across the fixed and suspended metal coated comb drive fingers. Additional suspended carbon nanotube is anchored and electrically contacted at two points by EBID lines. One anchor is on the movable NEMS comb drive structure and the other on the fixed counterpart. By applying an electrostatic force via the comb drive structure, the suspended structure can be displaced and thus a specific mechanical stress can be induced to the suspended CNT. This structure can be used as a test stand to study electromechanical properties of CNTs. With the help of EBID, electrical contacts can be made after the whole structure has been released, which is the case for CVD grown carbon nanotubes. For a proof of principle, we fabricated EBID leads on such a NEMS structure without a suspended CNT. Figure 6(b) shows half of the NEMS test structure with comb drive and springs. In Fig. 6(c) a closeup is given with EBID tungsten leads. Thus EBID can be successfully applied to these struc-

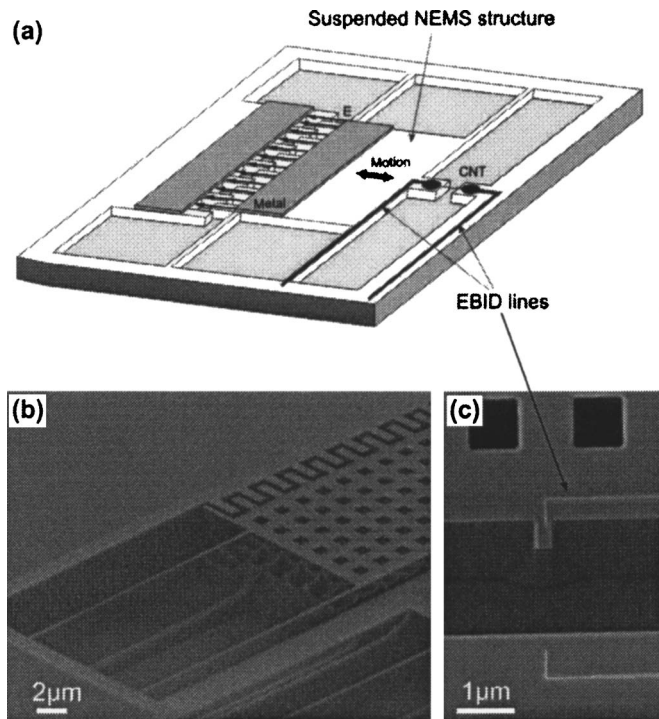


FIG. 6. (a) Schematic illustration of a NEMS device for mechanical and electromechanical measurements on CNTs. (b) NEMS structure consisting of suspended Al_2O_3 structures without and (c) with additional EBID leads.

tures, but the deposition conditions are less favorable with regards to precursor flux and sensitivity to charging and drift. However, with prepatterned gold electrodes, EBID based wiring of CNTs integrated in NEMS structures will be possible.

V. CONCLUSION AND OUTLOOK

A process for electrically connecting nanostructures with EBID was presented. This process can be used for randomly located nano-objects such as adsorbed CNTs and has the potential to connect suspended carbon nanotubes as part of NEMS. We electrically characterized the gold-EBID tungsten contact and obtained a resistivity of the EBID tungsten leads of $<10^{-2} \Omega \text{ cm}$. Electrical measurements showing

transistorlike behavior of CNTs prove the successful wiring of CNTs by EBID leads. Moreover the basic EBID process has been carried out on an alumina NEMS structures with freestanding 100 nm thick Al_2O_3 structures.

Next steps will include the combination of the EBID fabrication within NEMS and electrical measurements on CNTs. Therefore, we optimize the overall design of NEMS with coarse electrodes and EBID leads. Moreover, the contact resistance and the electrical characteristics of the EBID tungsten need to be further investigated and improved.

ACKNOWLEDGMENTS

The authors would like to thank A. Jungen, D. Obergfell, and R. Grundbacher for helpful discussions. Three of the authors (C.S., T.H., and C.H.) gratefully acknowledge financial support by the TH-18/03-1 Grant.

¹A. N. Cleland, *Foundations of Nanomechanics* (Springer, New York, 2003).

²H. G. Craighead, *Science* **290**, 1532 (2000).

³For review see, e.g., S. Reich, C. Thomsen, and J. Maultzsch, *Carbon Nanotubes* (Wiley-VCH, New York, 2003).

⁴M. L. Roukes, *Nanoelectromechanical Systems*, Technical Digest of the 2000 Solid-State Sensor and Actuator Workshop, Hilton Head Island, SC, 4–8 June 2000 (unpublished).

⁵S. W. Lee, D. S. Lee, R. E. Morjan, S. H. Jhang, M. Sveningsson, O. A. Nerushev, Y. W. Park, and E. E. B. Campbell, *Nano Lett.* **4**, 2027 (2004).

⁶M. Nishio, S. Sawaya, S. Akita, and Y. Nakayama, *Appl. Phys. Lett.* **86**, 133111 (2005).

⁷C. Stampfer *et al.*, *Nano Lett.* **6**, 233 (2006).

⁸N. R. Franklin, Q. Wang, T. W. Tomblor, A. Javey, M. Shim, and H. Dai, *Appl. Phys. Lett.* **81**, 913 (2002).

⁹A. Jungen, C. Stampfer, J. Hoetzel, V. Bright, and C. Hierold, *Sens. Actuators, A* **130–131**, 588 (2006).

¹⁰H. W. P. Koops, R. Weiel, D. P. Kern, and T. H. Baum, *J. Vac. Sci. Technol. B* **6**, 477 (1988).

¹¹M. D. Croitoru, G. Bertsche, D. P. Kern, C. Burkhardt, S. Bauerdick, S. Sahakalkan, and S. Roth, *J. Vac. Sci. Technol. B* **23**, 2789 (2005).

¹²T. Brintlinger *et al.*, *J. Vac. Sci. Technol. B* **23**, 3174 (2005).

¹³I. Utke, P. Hoffmann, B. Dwir, K. Leifer, E. Kapon, and P. Doppelt, *J. Vac. Sci. Technol. B* **18**, 3168 (2000).

¹⁴C. Stampfer, A. Jungen, and C. Hierold, *IEEE Sens. J.* **6**, 613 (2006).

¹⁵From CNI, Rice University, Houston, TX.

¹⁶M. K. Tripp *et al.*, *Sens. Actuators, A* **130–131**, 419 (2006).

¹⁷M. K. Tripp, C. Stampfer, C. F. Herrmann, C. Hierold, S. George, and V. M. Bright, *The 13th International Conference on Solid-State Sensors, Actuators, and Microsystems, Transducers 2005*, Seoul, Korea, 3–9 June 2005 (IEEE, New York, 2005), Vol. 1, pp. 851–854.